Ectopic Calcification is Caused by Elevated Levels of Serum Inorganic Phosphate in Mdx Mice

Namiko Kikkawa[1], Tomohisa Ohno[1], Yosuke Nagata[1], Masataka Shiozuka[1], Toshihiro Kogure[2], and Ryoichi Matsuda[1]*

[1]*Graduate School of Arts and Sciences, The University of Tokyo, 3-8-1 Komaba, Meguro-ku, Tokyo 153-8902, Japan* and [2]*Department of Earth and Planetary Science, Graduate School of Science, The University of Tokyo, 7-3-1 Hongo, Bunkyo-ku, Tokyo 113-0033, Japan*

ABSTRACT. **Ectopic calcification occurs in the skeletal muscle of mdx mice, a dystrophin-deficient animal model of Duchenne muscular dystrophy. The purpose of this study was to clarify the mechanism of the calcification. The calcified deposits were identified as hydroxyapatite, a crystallized form of calcium phosphate, and the serum inorganic phosphate (Pi) level in the mdx mice was approximately 1.4 times higher than that in the normal B10 mice, suggesting that Pi plays a critical role in the ectopic calcification. When C2C12 mouse myoblasts were cultured under high-Pi conditions, myogenic differentiation was retarded while the expression of osteogenic markers such as osteocalcin and Runx2 were upregulated. This was followed by the generation of calcium deposition. Moreover, ectopic calcification reduced to an undetectable level in most of the mdx mice fed a Pi-reduced diet. We therefore conclude that the Pi-induced osteogenesis of muscle cells is responsible for ectopic calcification in the skeletal muscle of mdx mice.**

Key words: ectopic calcification/inorganic phosphate/mdx mouse/muscular dystrophy/skeletal muscle

Introduction

Duchenne muscular dystrophy (DMD) is a progressive and genetic muscle disorder which leads to cardiac or respiratory failure resulting in the death of affected individuals by their late 20 s. DMD is caused by mutations in the dystrophin gene (Hoffman *et al*., 1987). Dystrophin is the central component of the dystrophin-associated protein complex (DPC), which stabilizes the sarcolemma by forming a link between the actin cytoskeleton and laminin, an extracellular matrix protein (Ervasti *et al*., 1990; Blake *et al*., 2002). In the skeletal muscle of DMD patients and mdx mice, the ani-

mal model of DMD (Bulfield *et al*., 1984), dystrophin is virtually absent. Dystrophin deficiency increases membrane fragility, which renders muscle fibers susceptible to damage during contraction (Petrof *et al*., 1993, Matsuda *et al*., 1995).

Ectopic calcification has been reported in various soft tissues such as the skin, kidney, tendons and blood vessels under pathological conditions (Giachelli, 1999). Calcification of the skeletal muscles in mdx mice and dystrophic dogs has also been reported (Geissinger *et al*., 1990; Nguyen *et al*., 2002), although its mechanisms remain entirely unclear. Calcification of cardiovascular tissue has been especially well studied for its clinical consequences, as vascular calcification in dialysis patients is associated with morbidity and mortality (Ketteler *et al*., 2005). The inappropriate biomineralization of blood vessels had been regarded as a passive process caused by calcium phosphate precipitation (Schinke and Karsenty, 2000). However, within the last decade it has been suggested that vascular calcification is actively regulated by osteogenic gene expression in vascular smooth muscle cells (Giachelli, 1999). Attention has been focused on inorganic phosphate (Pi) as one of the factors regulating the observed cellular phenotypic changes, as cells cultured under high-Pi conditions undergo osteogene-

*To whom correspondence should be addressed: Ryoichi Matsuda, University of Tokyo, Room 309A, Building 15, 3-8-1 Komaba, Meguro-ku, Tokyo 153-8902, Japan.

Tel: +81–3–5454–6637, Fax: +81–3–5454–4306

E-mail: cmatsuda@mail.ecc.u-tokyo.ac.jp

Abbreviations: 3-D: 3-dimensional; BMP-2: bone morphogenetic protein-2; CT: computed tomography; DMD: Duchenne muscular dystrophy; DMEM: Dulbecco's modified Eagle's medium; DPC: dystrophin-associated protein complex; GAPDH: glyceraldehyde-3-phosphate dehydrogenase; EDS: energy-dispersive X-ray spectrometry; FGF-23: fibroblast growth factor-23; HA: hydroxyapatite; MyHC: myosin heavy chain; PBS: phosphate buffered saline; Pi: inorganic phosphate; SEM: scanning electron microscopy; TEM: transmission electron microscopy

sis and form calcium depositions *in vitro* (Jono *et al.*, 2000).

The main objective of this study was to uncover the nature of calcification in mdx mouse skeletal muscle. Since muscle satellite cells possess multilineage potential (Asakura *et al.*, 2001; Wada *et al.*, 2002), we tested the hypothesis that the osteogenesis of muscle cells is the key cause of ectopic calcification in mdx mice.

Materials and Methods

Animal care and dietary treatment

Mdx and normal C57BL/10 mice, provided by the National Center of Neurology and Psychiatry (Japan), were kept at 25°C under a 12 h light-dark cycle in a conventional animal-care facility. A low Pi diet (0.1% Pi instead of 0.9% Pi in normal diet) was manufactured by Oriental Yeast (Tokyo, Japan). For Pi uptake restriction, the mice were fed the low Pi diet during lactation and after weaning until reaching 2 months of age. The animals were euthanized with an overdose of ether gas. The animal experiments were carried out according to the animal experimental manual of the University of Tokyo.

Antibodies

The primary antibodies used were as follows: anti-sarcomeric myosin heavy chain (MyHC) mouse monoclonal antibody MF20 (Developmental Studies Hybridoma Bank, University of Iowa, Iowa City, Iowa), mouse monoclonal anti-myogenin antibody F5D (Developmental Studies Hybridoma Bank), rabbit polyclonal anti-Runx2 (transcription factor expressed during osteogenesis) antibody (Santa Cruz Biotechnology, Santa Cruz, CA) and rat polyclonal anti-F4/80 (glycoprotein expressed by mature macrophages) antibody (Serotec, Oxford, UK). The secondary antibodies used for immunohistochemistry were Alexa Fluor 488-conjugated goat anti-mouse IgG, Alexa Fluor 488-conjugated goat anti-rat IgG and Alexa Fluor 594-conjugated goat anti-rabbit IgG (Invitrogen, Carlsbad, CA); those for Western blotting were IRDye 800-conjugated goat anti-mouse IgG (Rockland, Gilbertsville, PA) and Alexa Fluor 680-conjugated goat anti-rabbit IgG (Invitrogen). All diluted antibodies were centrifuged at $15,000 \times g$ for 5 min prior to use in order to eliminate aggregates.

X-ray micro CT observation

The lower limbs of mdx and B10 mice were excised and wrapped in NOVIX parafilm (AGC Techno Glass, Chiba, Japan), mounted on the stage with plasticine, and scanned using the high-resolution X-ray micro-computed tomography (CT) SkyScan-1074 scanner (SkyScan, Kontich, Belgium) operated at 40 kV and 1000 μA. X-ray transmission images were acquired from a longitudinal view rotated every 0.9-degrees under a 660-msec exposure. CT images at a resolution of 22 μm were reconstructed using cone-beam reconstruction software (SkyScan) before 3-dimensional (3-D)

images were generated with the image analysis software CTAn (SkyScan). Calcification was quantified using the 3-D analysis software CTVol (SkyScan). After the CT analysis, calcified areas of mdx mice were fixed with 10% formalin in phosphate buffered saline (PBS) for further X-ray analysis or embedded in OCT compound (Sakura Finetechnical, Tokyo, Japan) before being frozen in liquid nitrogen-cooled melting isopentane. Transversal cryosections with 5 μm thickness were prepared for von Kossa, alizarin red S and immunofluorescent stainings. Von Kossa stained samples were counterstained with nuclear fast red. For whole-body imaging, mdx mice were deeply anesthetized by an intraperitoneal injection of pentobarbital (50 mg/kg body weight, Dainippon Sumitomo Pharma, Osaka, Japan) and subjected to X-ray micro CT scanning on a LaTheta LTC-100 (Aloka, Tokyo, Japan).

Scanning Electron Microscopy (SEM) and Transmission Electron Microscopy (TEM) analyses

Muscle calcification was identified by back-scattered electron imaging and energy-dispersive X-ray spectrometry (EDS) analysis of a piece of dried muscle coated with a thin carbon film using a S-4500 SEM (Hitachi, Tokyo, Japan) operated at 15 kV. The piece of muscle was also ground and suspended in ethanol, then dispersed on a holey carbon microgrid (Nissin EM, Tokyo, Japan) for TEM investigation. A JEM-2010 TEM (JEOL, Tokyo, Japan) equipped with an EDS detector was used to identify the mineral phase by analyzing the composition and electron diffraction pattern of the sample.

Measurements for Serum calcium, Inorganic Phosphate (Pi), and Fibroblast Growth Factor (FGF)-23

Mouse blood was collected via a retro-orbital sinus puncture and incubated overnight at 4°C. Serum was subjected to calcium and Pi measurements using the automated clinical chemistry analyzer Fuji Dri-chem 4000 (Fujifilm, Tokyo, Japan) based on colometric analysis using the chlorophosphonazo-III and purine nucleoside phosphorylase reactivity, respectively (Ferguson *et al.*, 1964; Hwang *et al.*, 1973). For FGF-23 measurements, mouse sera collected as described above were tested for FGF-23 concentration using an FGF-23 ELISA kit (Kainos Laboratories, Tokyo, Japan).

Cell cultures

C2C12 mouse myoblasts were cultured in a growth medium (high-glucose Dulbecco's modified Eagle's medium (DMEM: Gibco, Grand Island, NY) containing 20% fetal bovine serum (JRH Biosciences, Lenexa, KS), 50 IU/ml penicillin, and 50 μg/ml streptomycin (Gibco)). The cells were trypsinized before reaching confluency and reseeded at an initial density of 1×10^4 cells/cm^2 in gelatin-coated Petri dishes (AGC Techno Glass, Chiba, Japan). After 24 h incubation, the growth medium was replaced with differentiation medium (DMEM containing 2% horse serum (Gibco) and penicillin-streptomycin). For the primary culture, cells were prepared from the mdx mouse rectus femoris muscle by 0.5%

trypsin digestion, resuspended in primary culture medium (DMEM containing 20% fetal bovine serum, 10% horse serum and penicillin-streptomycin) and then seeded in gelatin-coated Petri dishes. The differentiation medium and the primary culture medium contained 1.0 mM and 1.3 mM of Pi, respectively. For the induction of calcification, the media were supplemented with Pi solution (NaH2PO4-Na2HPO4, pH 7.4) to a final concentration of 3~9 mM. Likewise, 5 mM of Pi and 2 mM of calcium chloride were added to the differentiation medium to enhance calcium phosphate deposition. The cells were cultured at 37°C and 5% CO_2 in a humidified atmosphere.

Quantification of calcium deposition

C2C12 cells seeded in 24-well plates (AGC Techno Glass) were cultured as described above. After fixation with 10% formalin in PBS for 30 min at room temperature, the cells were washed 3 times in PBS and treated with a 2N HCl solution overnight at room temperature to dissolve the calcium depositions. The calcium concentration of the supernatant was measured using the Calcium E-test (Wako Pure Chemical Industries, Osaka, Japan) based on the *o*-cresolphthalein complexone method (Gindler and King, 1972). After the calcium measurement, the cells were washed 3 times in PBS, lysed in 125 mM Tris-HCl (pH 6.8) with 2% SDS for 10 min on ice, and the protein concentration of the supernatant was then determined using BCA Protein Assay Reagent (Pierce, Rockford, IL). The absorption at 595 nm was observed on a Model 680 Microplate Reader (Bio-Rad, Hercules, CA) for both assays. The calcium content was normalized to the total protein content in each well.

Immunofluorescent staining

Muscle tissue cryosections 5 μm in thickness were fixed with 10% formalin in PBS for 30 min at room temperature. The cultured cells were subjected to the same procedure, but were treated with 0.5% Triton X-100 (ICN Biochemicals, Aurora, OH) in PBS to permeabilize the cell membrane before incubation with the primary antibody. The samples were reacted with the primary antibody overnight, followed by washing 3 times in PBS. The secondary antibody was applied to the section for 1 h at room temperature and washed again 3 times in PBS. Five μg/ml of Hoechst 33258 (Sigma Aldrich, St. Louis, MO) was added to the secondary antibody solution to visualize the nuclei. For the negative controls, the primary antibody was replaced with PBS. All antibodies were appropriately diluted in PBS containing 0.5% bovine serum albumin (Sigma Aldrich).

The fusion index, defined as the ratio of the nuclei in multi-nuclear myotubes to all the nuclei, was used as a marker of muscle differentiation. More than 600 nuclei were counted for each sample.

Western blot analysis

C2C12 cells were fixed with 10% trichloroacetic acid (Wako Pure Chemical Industries) in PBS for 30 min at 4°C, rinsed 3 times with ice-cold PBS, scraped off the plate, and then collected by centrifugation at 15,000×*g* for 5 min. The pellets were lysed by sonication in sample buffer (125 mM Tris-HCl and 2% SDS, pH adjusted to 6.8). The total protein concentration of the lysates was determined using BCA Protein Assay Reagent (Pierce, Rockford, IL) and adjusted to an equal concentration before boiling for 5 min in the presence of 0.1 M DTT (Wako Pure Chemical Industries). The proteins were subjected to 18% SDS-PAGE and transferred to an Immobilon-FL PVDF membrane (Millipore, Billerica, MA). After incubating in Odyssey Blocking Buffer (LI-COR Biosciences, Lincoln, NE) for 2 to 4 h, the membranes were probed with primary antibody overnight at room temperature. The membranes were washed 3 times in PBS containing 0.5% Tween 20 (ICN Biochemicals), followed by a 1 h incubation with the secondary antibody, and again washed 3 times in PBS/Tween 20. All antibodies were diluted in Odyssey Blocking Buffer. The protein bands were visualized using the Odyssey Infrared Imaging System (LI-COR Biosciences) which allows multiplex detection; thus, an objective protein and an internal loading control can be detected on the same membrane at the same time.

RT-PCR

RNA samples were collected from C2C12 cells using RNA-Bee (IsoTex Diagnostics, Friendswood, TX) and reverse transcription was performed using the First Strand cDNA Synthesis Kit (Marligen Biosciences, Ijamsville, MD) according to manufacturers' protocols. PCR amplification was carried out with Premix Taq (Takara Bio Inc, Shiga, Japan). Primer sequences of osteocalcin (forward: 5'-CAA GTC CCA CAC AGC AGC TT-3', reverse: 5'-AAA GCC GAG CTG CCA GAG TT-3') and glyceraldehyde-3-phosphate (GAPDH, forward: 5'-GTG AAG GTC GGA GTC AAC G-3', reverse: 5'-GGT GAA GAC GCC AGT GGA CTC-3') were obtained from previous studies (Desbois *et al*., 1994; Ploszaj *et al*., 1998).

Results

X-ray micro CT observation

The hind limbs of mdx and B10 mice at various ages were scanned with an X-ray micro CT scanner (Fig. 1). Fig. 1A shows representative images of the hind limb from a 2-month-old mdx mouse. The bony structure in the middle of the X-ray transmission image is the femur. X-ray-absorbing particles aligned towards the direction of muscle fibers were found in the skeletal muscle tissues by CT (Fig. 1A-CT), but were barely observable in the X-ray transmission image. Ninety-two percent of mdx mice exhibited these particles (n=12), while no such structures were observed in B10 mice (Fig. 1B, n=8). The particles found in the mdx mice were also detectable non-invasively using the whole-body X-ray micro CT scanner LaTheta LTC-100 (Fig. 1C).
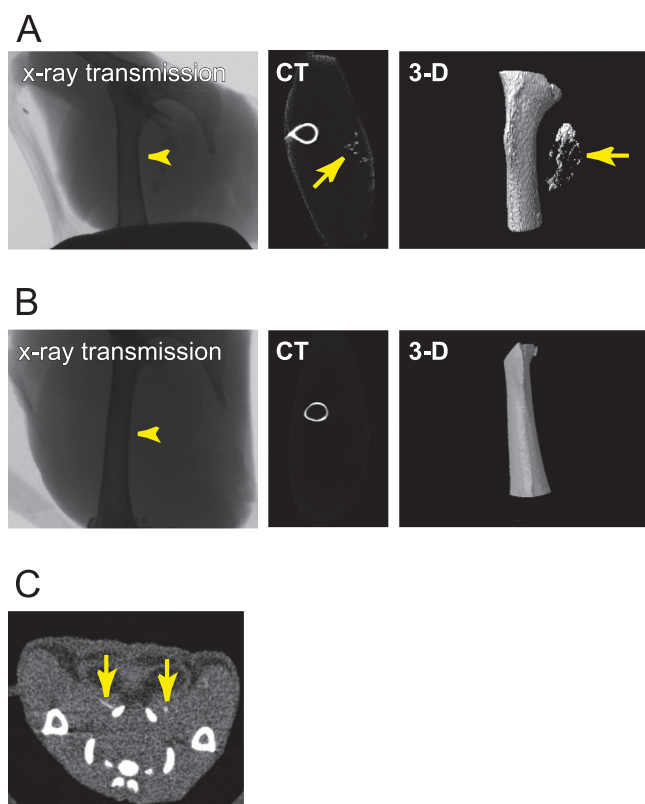
Fig. 1. (A) Images of the hind limb of a 2-month-old mdx mouse, obtained using the X-ray micro CT scanner SkyScan 1074. X-ray transmission image: X-ray-absorbing materials are shown as gray shadows, and the femur (indicated by the arrowhead) can be seen in the middle of the X-ray. CT image: the grayscale was inverted, and the X-ray-absorbing substances are shown in white. The white loop in the middle signifies the femur. X-ray-absorbing particles (indicated by the arrow) apparently differing from bone can be observed. Reconstructed 3-D image: X-ray-absorbing particles (indicated by the arrow) are distributed parallel to the femur in skeletal muscle tissue of the mdx mouse. (B) Images of the hind limb of a 2-month-old B10 mouse obtained using the X-ray micro CT scanner SkyScan 1074. The femur is indicated by the arrowhead. No calcification was observed in the X-ray transmission, CT and 3-D images. (C) A CT image of the lower abdomen of a mdx mouse obtained using the whole-body X-ray micro CT scanner LaTheta LTC-100. The X-ray-absorbing particles are indicated by arrows.

Identification of the mineral phase by SEM and TEM

Fig. 2A shows a back-scattered electron image obtained by SEM from a cross-section of the muscle from the hind-limb of an mdx mouse. Some muscle bundles displayed a bright contrast, corresponding to a large atomic number. The EDS spectra obtained from these brightly-contrasted bundles indicated the presence of both calcium and phosphorus, which suggested the formation of a calcium phosphate phase (data not shown). To determine the mineral phase, the specimen was further analyzed using TEM. Fig. 2B is a TEM image of the calcium-containing material, and the

electron diffraction pattern from the material within the white circle in Fig. 2B is shown in Fig. 2C (top-left and bottom-right). A simulation of the diffraction pattern (Fig. 1C, top-right and bottom-left) using the crystallographic parameters of hydroxyapatite (HA, $Ca_5(PO_4)_3OH$) showed an almost identical match between the observed and simulated electron diffraction patterns. This indicates that the observed calcification of the muscle was due to a precipitation of HA particles. The EDS spectrum (Fig. 2D) taken from the sample within the white circle in Fig. 2B also confirmed the presence of calcium and phosphorus, providing strong evidence that the material was indeed HA. Therefore, these particles are hereafter referred to as "ectopic calcification."

Histological staining

A cryosection of 2-month-old mdx mouse skeletal muscle was von Kossa-stained to confirm the presence of calcium (Fig. 3A). Von Kossa-positive particles were observed, suggesting that they consisted of calcium. Other cryosections were stained with alizarin red S or antibodies for F4/80 (Fig. 3B). The calcified areas stained dark red (Fig. 3B-a) and the serial section, washed gently under running water beforehand, was also positively-stained (Fig. 3B-b). Some of the muscle fibers were alizarin red S-positive when stained without the pre-washing procedure (Fig. 3B-d); however, after washing they turned negative (Fig. 3B-e). We presumed that in these particular fibers, calcium ions had accumulated prior to calcium deposition in the form of HA particles.

Another set of serial sections were immunostained for F4/80, a transmembrane protein expressed in macrophages and widely used as a macrophage marker. Macrophage accumulation was observed in the areas surrounding calcification (Fig. 3B-c) and in calcium-rich muscle fibers (Fig. 3B-f). No alizarin red S-positive fibers were observed in the B10 mice before (Fig. 3B-g) or after washing (Fig. 3B-h). Macrophage accumulation (Fig. 3B-i) was not detected in the B10 mice.

Serum Calcium, Pi, and FGF-23 measurement

As we confirmed that ectopic calcification is composed of HA, a major form of calcium phosphate in vertebrates, a metabolic disorder of calcium or phosphate was suspected in the mdx mice. The serum Pi and calcium levels in mdx and B10 mice at 2 months of age were compared (Fig. 4). While no significant difference in serum calcium was observed between the B10 and mdx mice, the serum Pi level of the mdx mice was significantly higher compared to that of the B10 mice. These results were consistent with a previous study by Brazeau *et al.* (1992). The serum level of FGF-23, a protein which regulates serum phosphate level by suppressing renal Pi absorption, was also measured in the
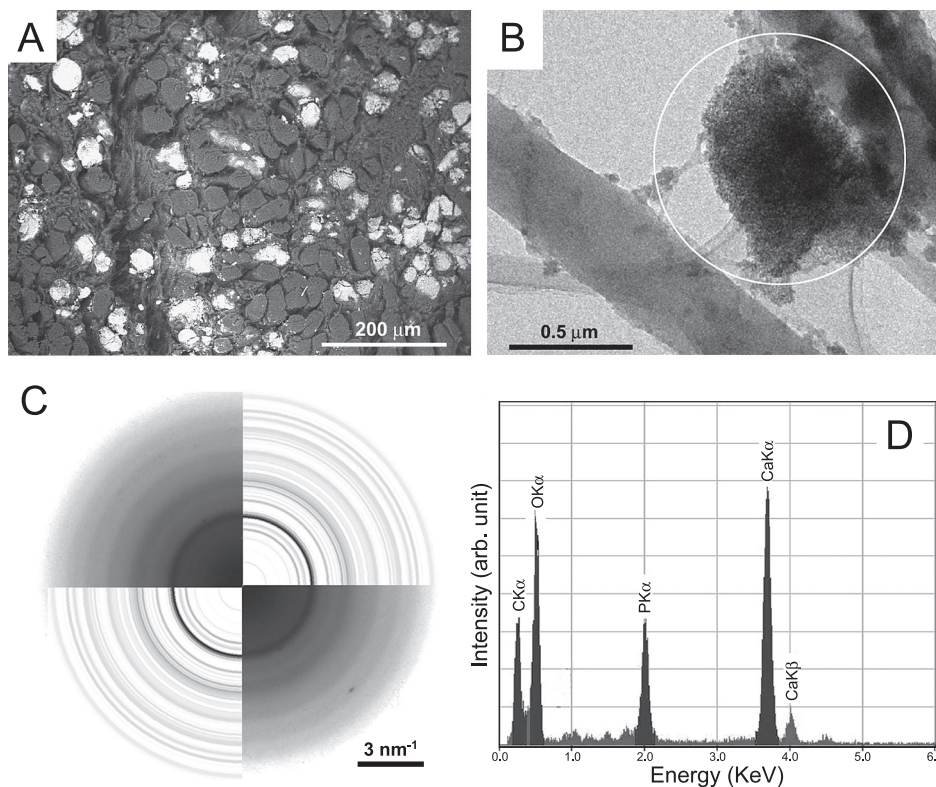
Fig. 2. (A) Back-scattered SEM image from a cross-section of mdx skeletal muscle. The calcified muscle bundles are shown in bright contrast. (B) TEM image of ground mdx skeletal muscle. Inorganic material can be observed between the muscle fibers. (C) Electron diffraction pattern (top-left and bottom-right) from within the white circle in (B) and the simulated pattern for hydroxyapatite (HA) (top-right and bottom-left). (D) EDS spectrum obtained from the material within the white circle in (B).

2-month-old B10 and mdx mice. The serum FGF-23 concentration of mdx mice was significantly higher than in the B10 mice (Fig. 4).

Detection of Pi-induced osteogenesis in C2C12 cells

To study the effects of Pi in muscle cell differentiation, murine myoblast-derived C2C12 cells were cultured for 4 days under various Pi concentrations and immunostained for the presence of myogenic and osteogenic markers (Fig. 5A–C). The cells underwent muscle differentiation and formed myotubes when cultured in normal differentiation medium (Pi=1 mM). Myogenesis proceeded until the Pi concentration of the differentiation medium reached 5 mM, but myotube formation was strongly suppressed at 7 mM (Fig. 5A). The retardation of myogenesis caused by the high Pi concentration was also evident by the decrease in the fusion index and myogenin expression (Fig. 5B). The expressions of Runx2, a transcription factor of osteogenesis and used as an osteogenic marker, increased with the rise of the Pi concentration (Fig. 5B). It is notable that under the condition of 5 mM Pi, myogenesis was not inhibited and the cells differentiated into myotubes, while the expression of

Runx2 was augmented. Further observation revealed that myogenin and Runx2 did not colocalize in the same nuclei. Runx2 expression in the myotubes was observed not in the nuclei, but in the cytoplasm (Fig. 5C). This suggests that Runx2 is inactive in myogenic cells, as it has been reported that Runx2 activity is regulated by translocation between the nucleus and the cytoplasm (Zaidi *et al*., 2001).

Likewise, upregulation of Runx2 expression was observed by Western blotting not only when the cells were cultured under high-Pi conditions, but also when cultured in the presence of calcium phosphate deposits, which were generated by the addition of sodium phosphate and calcium chloride to the medium (Fig. 5D).

To study the expression of osteocalcin, a secreted protein whose expression is regulated by Runx2 (Xiao *et al*., 1999) and used as another marker for osteogenesis, RT-PCR was performed with RNA samples prepared from C2C12 cells cultured under various Pi concentrations for 4 days. Osteocalcin expression was undetectable when the cells were cultured with 1 mM Pi, but increased with the elevation of the Pi concentration (Fig. 5E).

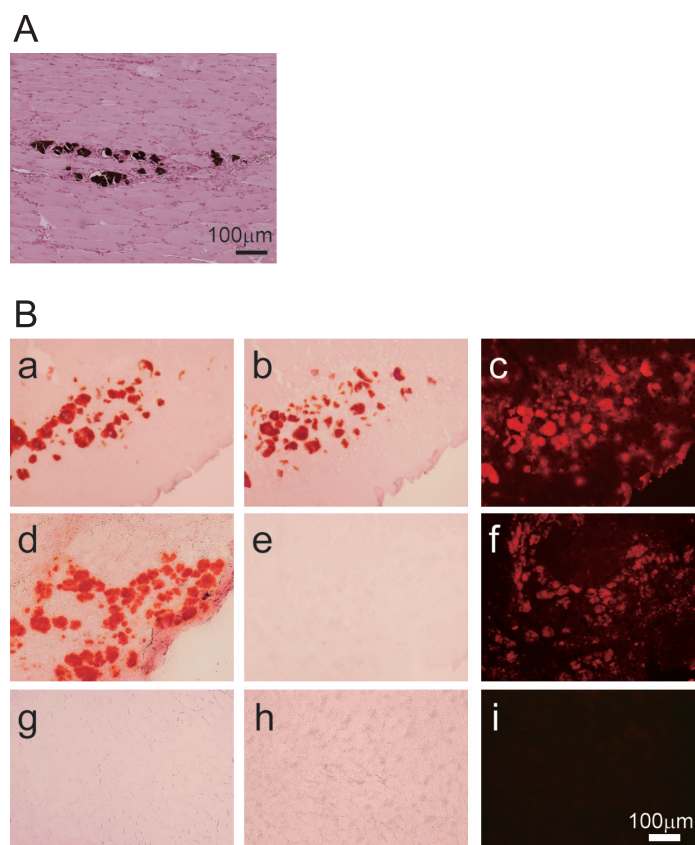The calcium deposition in C2C12 cells cultured under various Pi concentrations was measured and normalized to

Fig. 3. Von Kossa, alizarin red S-stained and immunostained cryosections of mdx and B10 mice skeletal muscle. (A) Von Kossa-stained section of a 2-month-old mdx mouse hind limb. The X-ray-absorbing particles detected by the X-ray micro CT scanner are stained black. (B-a, d) Alizarin red S-stained cryosections of mdx mouse skeletal muscle. The calcified or calcium-rich areas are stained red. (B-b, e) Serial sections of (B-a) and (B-d) stained with alizarin red S after washing with tap water. The calcified areas were stained red (B-a), and remained alizarin red S-positive after washing (B-b). There were some muscle fibers which were alizarin red S-positive before washing (B-d), but turned negative after washing (B-e). These fibers are presumed to contain high concentrations of calcium ions and are undergoing calcification. (B-c, f) Another set of serial sections of (B-a) and (B-d) were immunostained for F4/80. Macrophages are accumulated in both regions. (B-g, h) Alizarin red S-stained cryosections from a B10 mouse before (B-g) or after (B-h) washing. No positive fibers were observed. (B-i) Serial section of (B-g) immunostained for F4/80. No macrophage accumulation was observed.
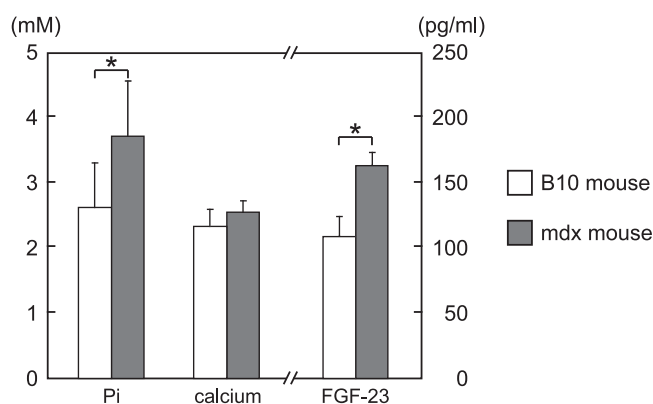

Fig. 4. Serum Pi and calcium levels of B10 and mdx mice at 2 months of age. The serum Pi concentration of mdx mice was 1.41 times higher than in B10 mice, while no significant difference was observed in the calcium concentration between the 2 strains. The serum FGF-23 concentration of mdx mice was 1.5 times higher than in B10 mice. (*: $p < 0.05$)

the corresponding protein content at day 7 (Fig. 6). The cells did not deposit calcium under normal Pi conditions, whereas the cells cultured in medium containing 3 mM of Pi or higher deposited calcium. The amount of calcium increased significantly at higher Pi concentrations.

Pi-induced calcification in the primary culture of skeletal muscle cells

Cells isolated from mdx skeletal muscle tissue were cultured in normal Pi (1.3 mM) or high-Pi (5 mM) medium to study the effects of Pi in primary culture cells (Fig. 7). The cells formed myotubes when cultured in normal medium, while myotube formation was strongly inhibited under high-Pi conditions. Both alizarin red S staining and von Kossa staining revealed that numerous calcium deposits were present after 10 days of culture in high-Pi medium, but were not detected in cells cultured in normal medium.
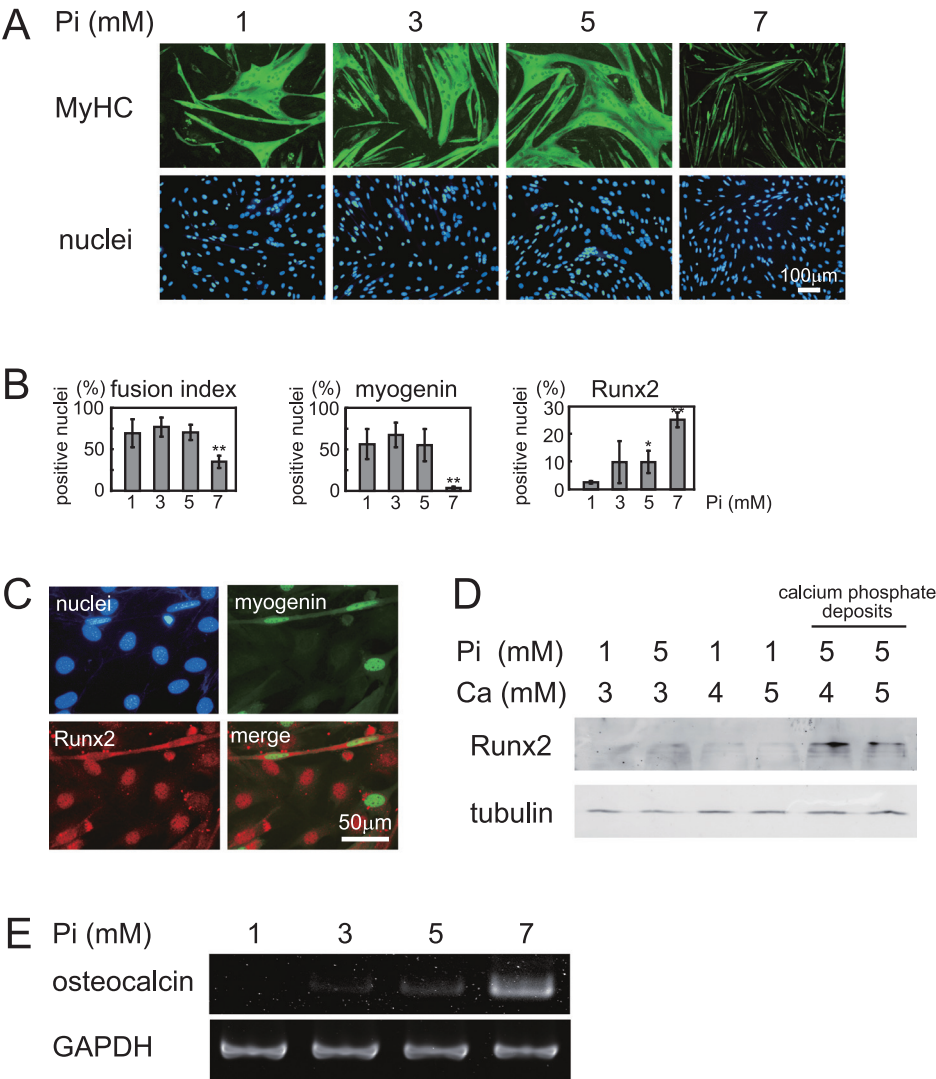
Fig. 5. Immunocytochemistry and RT-PCR of C2C12 cells cultured under various Pi concentrations. The Pi concentration of each condition was 1, 3, 5, and 7 mM. (A) Cells immunostained for MyHC (green). MyHC-positive myotubes formed at 1, 3 and 5 mM Pi but were completely absent at 7 mM. Nuclei were stained with Hoechst 33258 (blue). (B) The myogenin expression, the fusion index, and the expression of Runx2 were quantified. The fusion index and ratio of the nuclei expressing myogenin decreased, while the ratio of Runx2-expressing nuclei increased with increasing Pi concentration. (*: $p<0.05$; **: $p<0.01$). (C) Close observation of cells cultured in medium containing 5 mM of Pi, stained with Hoechst 33258 to show the nuclei or immunostained for myogenin or Runx2. The cells did not express myogenic and osteogenic markers at the same time. (D) Western blotting of C2C12 cells cultured under increased Pi or calcium concentrations. Runx2 expression was enhanced when the cells were co-cultured with calcium phosphate deposits. (E) RT-PCR for osteocalcin in C2C12 cells cultured in media containing 1, 3, 5, and 7 mM Pi. Osteocalcin mRNA was not detected at 1 mM Pi but increased with increasing Pi concentrations. GAPDH was used as an internal control.
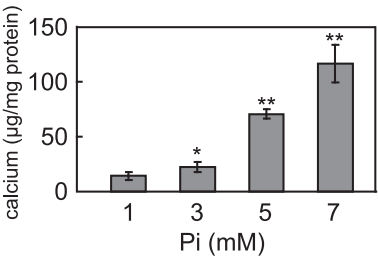

Fig. 6. Quantification of calcium deposits generated by C2C12 cells cultured under various Pi concentrations. Calcium deposition increased with increasing Pi concentrations. No calcification was observed in cells culture under normal conditions. (*: $p<0.05$, **: $p<0.01$.)
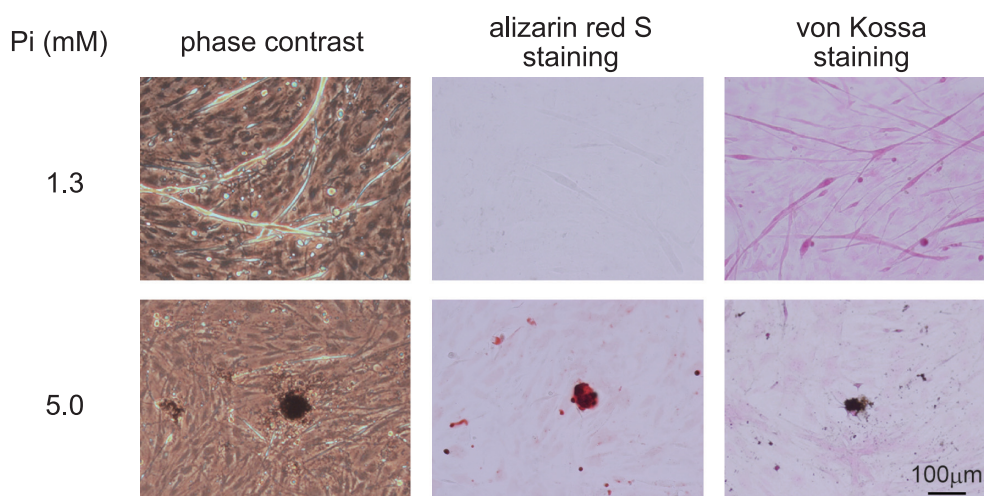
Fig. 7. Calcification of mdx mouse muscle-derived primary culture cells. Cells were cultured for 10 days at a Pi concentration of 1.3 mM or 5 mM. Calcium depositions were stained red or black with alizarin red S and von Kossa staining, respectively, while no calcification was observed when the cells were cultured in normal medium containing 1.3 mM of Pi. The von Kossa-stained samples were counterstained with nuclear fast red, and the myotubes were stained pink.
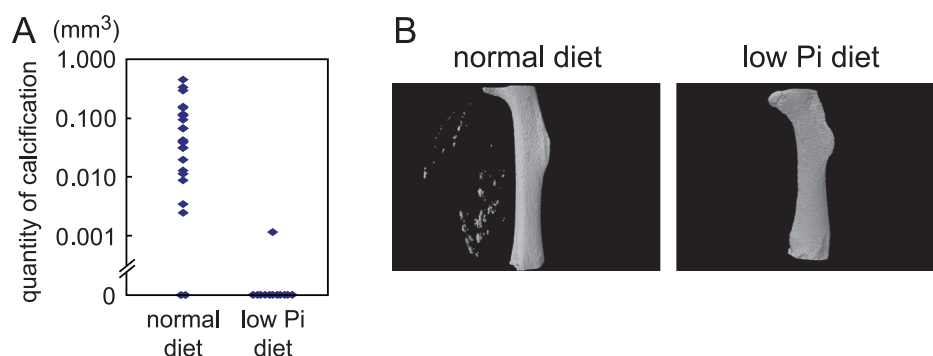

Fig. 8. Inhibition of ectopic calcification in mdx mice by a low Pi diet. (A) Quantity of ectopic calcification observed in mdx mice fed a normal or low Pi diet for 2 months. The mass of calcification per 1 hind limb significantly decreased when mice were fed the low Pi diet. (B) Reconstructed 3-D images of the hind limb of an mdx mouse fed a normal or low Pi diet. Ectopic calcification, which was observed in mdx mice fed the normal diet, disappeared in 83% of the hind limbs of mdx mice fed the low Pi diet.

Inhibition of ectopic calcification in mdx mouse skeletal muscle by a low Pi diet

To investigate the role of Pi in ectopic calcification *in vivo*, mice were fed a low Pi diet for 2 months. Serum Pi level decreased in both B10 (1.6 ± 0.13 mM) and mdx mice (2.1 ± 0.51 mM), and the restriction of Pi intake seemed to correct serum Pi elevation in mdx mice. However, the serum calcium level was elevated in both B10 (3.5 ± 0.25 mM) and mdx mice (3.0 ± 0.08 mM).

A low Pi diet also inhibited ectopic calcification in mdx mouse skeletal muscle (Fig. 8). The quantity of ectopic calcification of 2-month-old B10 and mdx mice in each diet group (n=6) was determined. Fig. 8A shows the mass of calcification per one hind limb of the mdx mouse fed a normal or low Pi diet. Ectopic calcification was observed in all hind limbs of the mdx mice fed with normal diet. However, calcification was undetectable in 5 out of 6 (83%) of the mdx mice fed a low Pi diet (Fig. 8B), and one mouse showed small-scale calcification in one of the hind limbs, whose quantity was decreased 78-fold compared to the average of the mdx mice fed with normal diet. B10 mice exhibited no calcification in either diet groups. No significant difference was observed in the body weight or survival rate between both diet groups of the B10 or mdx mice (data not shown).

Discussion

Ectopic calcification of skeletal muscle and serum Pi elevation in mdx mice

Ectopic calcification was observed in mdx mouse skeletal muscle, and was determined to be composed of hydroxyapatite (HA). As HA consists of calcium phosphate, it was assumed that the observed ectopic calcification was related to an aberration of calcium or Pi metabolism. The measurement of the serum calcium and Pi concentrations revealed that, while no significant difference was found in the calcium concentration, the Pi level in mdx mice was 1.4-fold higher than in the B10 mice.

It has been demonstrated that an increase in the extracellular Pi level in culture medium promotes mineralization in osteoblasts (Murshed *et al*., 2005) and vascular smooth muscle cells (Jono *et al*., 2000). Furthermore, ectopic calcification in soft tissues has been observed in mouse models exhibiting hyperphosphatemia: mice lacking alpha-Klotho (Kuro-o *et al*., 1997) or FGF-23 (Sitara *et al*., 2004). We hypothesized that skeletal muscle cells also undergo osteogenic differentiation under high-Pi conditions, leading to ectopic calcification in the skeletal muscle of mdx mice. To test this hypothesis, we cultured murine myoblast C2C12 cells in medium containing various concentrations of Pi.

Pi-induced osteogenesis and inhibited myogenesis in skeletal muscle cells

Skeletal muscle cells by nature maintain multi-lineage potential, and satellite cells are capable of adipogenic and osteogenic differentiation (Asakura *et al*., 2001; Wada *et al*., 2002). The C2C12 muscle cell line, derived from adult C3H mouse skeletal muscle, also possesses the properties of satellite cells (Yaffe and Saxel, 1977; Blau *et al*., 1983). C2C12 cells are capable of adipogenic or osteogenic differentiation under certain inducing conditions, such as supplementing the medium with gamma-linolenic acid to induce adipogenesis, and BMP-2 to induce osteogenesis (Wada *et al*., 2002; Katagiri *et al*., 1994).

The present results indicate that C2C12 cells cultured under high-Pi conditions expressed Runx2 and osteocalcin, and generated calcium deposits, which are typical of osteoblastic cells. The Pi-induced osteogenesis in C2C12 cells followed by calcium deposition observed in this study may reflect ectopic calcification in mdx mouse skeletal muscle.

The mechanisms by which extracellular Pi induces calcification in both osteogenic and non-osteogenic cells are not fully understood. However, it has been reported that Pit-1, one of the type-III sodium-dependent phosphate cotransporters, is necessary for increasing Pi uptake and consequently the Pi-induced expression of osteocalcin, osteopontin and other bone-related proteins during calcification in osteoblasts and vascular smooth muscle cells

(Li and Giachelli, 2007; Yoshiko *et al*., 2007). It has been reported that BMP-2 promotes Pit-1 expression, Pi uptake and calcification in vascular smooth muscle cells, suggesting that vascular calcification shares a common mechanism with physiological calcification (Li *et al*., 2008). Similar regulatory mechanisms may be involved in ectopic calcification in mdx mice.

In this study, the elevation of the medium Pi concentration not only induced osteogenesis but also led to the inhibition of myogenesis in C2C12 cells, which was evidenced by the attenuation of myotube formation and the decrease in the ratio of cells expressing myogenin. Myogenin regulates various genes necessary for skeletal muscle differentiation, including the expression of myosin heavy chain, troponin and another muscle-specific transcription factor, MRF4 (Perry and Rudnick, 2000; Davie *et al*., 2007). Interestingly, while osteogenic markers started to appear at a Pi concentration of 3~5 mM, the inhibition of myogenesis manifested in a decrease of the fusion index, and myogenin expression was not observed until the Pi concentration reached 7 mM. The difference in susceptibility to the Pi concentration between the inhibition of myogenesis and the facilitation of osteogenesis may explain the status of mdx skeletal muscle; both myogenesis and osteogenesis proceed at 5 mM Pi, the same concentration as the serum Pi in mdx mice. The immunocytochemistry of C2C12 cells indicated that myogenesis and osteogenesis are mutually exclusive; i.e., they do not occur simultaneously in the same cell. When the Pi concentration was elevated to 5 mM, the ratio of Runx2-positive cells increased while that of myogenin-expressing cells remain unchanged. This suggests that it was the reserve cells uncommitted to myogenesis which became Runx2-positive and proceeded with the osteogenic cascade under high-Pi conditions.

Calcium phosphate deposit-induced osteogenesis in myoblasts

In this study, we demonstrated that the ability of insoluble calcium phosphate to induce osteogenesis is higher than that of soluble Pi, as the expression of Runx2 in C2C12 cells was significantly upregulated when the cells were cultured in the presence of calcium phosphate deposits. This result is consistent with previous studies, in which mesenchymal stem cells and C2C12 cells co-cultured with HA crystals showed osteogenic differentiation (Damien and Parsons, 1991; Tan *et al*., 2007). The observation that the osteoinductive potential of calcium phosphate deposits is stronger than that of Pi suggests that ectopic calcification in mdx mouse skeletal muscle forms a positive feedback loop; once a calcium phosphate deposit is formed, it induces osteogenesis in adjacent cells and amplifies calcification in the surrounding areas.

Calcification independent of osteogenesis

In addition to osteogenesis-induced calcification, there may be a passive process of calcification formation: the development of calcium phosphate deposition in the presence of high concentrations of Pi and calcium ions. It is well known that calcium regulation is disrupted in dystrophin-deficient muscle, and that calcium ions accumulate in the cytosol of degenerating muscle fibers in mdx mice (Berchtold *et al.*, 2000; Gillis, 1999). The muscle fibers of mdx mice which were alizarin red S-positive but became negative after rinsing in running water were likely rich in calcium ions, as alizarin red S binds not only to calcium salts but also to calcium ions in the soluble state, which form visible precipitates (Lievremont *et al*., 1982). Though these muscle fibers are assumed to become mineralized, it is unlikely that cells first differentiate into myotubes and then re-differentiate into osteoblastic cells. Likewise, the immunohistochemistry of C2C12 cells revealed that Runx2 was not expressed in the nuclei of myotubes, suggesting that Runx2 is inactivated in these cells. Therefore, ectopic calcification not triggered by osteogenesis can be expected to occur in calcium-rich muscle fibers by the generation of calcium phosphate deposits.

Relationship between serum Pi and ectopic calcification in mdx mouse skeletal muscle

Since hyperphosphatemia and vascular calcification in FGF-23 null mice were corrected by a Pi-deficient diet (Stubbs *et al*., 2007), ectopic calcification in mdx mouse skeletal muscle may also decrease by feeding mdx mice a low-Pi diet. To investigate the involvement of Pi in ectopic calcification of mdx mouse skeletal muscle, dietary reduction of Pi was performed for 2 months.

A low-Pi diet significantly lowered serum Pi levels in both B10 and mdx mice, and the serum Pi of mdx mice reached the same level as B10 mice fed a normal diet. In the mdx mice fed a low-Pi diet, ectopic calcification of skeletal muscle was markedly inhibited. These results are consistent with our hypothesis that elevated levels of serum Pi induces ectopic calcification in mdx mouse skeletal muscle. However, since raising the serum Pi of normal mice by a high-Pi diet does not promote calcification in any soft tissues (Murshed *et al.*, 2005), factors other than Pi may also be involved in ectopic calcification.

The reason why the serum Pi concentration in mdx mice is higher than in B10 mice is not clear. FGF-23 has recently gained attention as a negative regulator of serum Pi levels, and it was anticipated that a decrease in serum FGF-23 was the cause of serum Pi elevation. Contrary to our expectation, however, mdx mouse serum FGF-23 levels were approximately 1.5 times higher than in B10 mice, suggesting that the serum FGF-23 level was increased to facilitate Pi exhaustion and to reduce the serum Pi level. The involve-

ment of other Pi-regulating factors, such as vitamin D, has yet to be clarified. It is possible that Pi leaks from damaged fibers into the circulation, as the intracellular Pi concentration of mdx mouse skeletal muscle during exercise is elevated compared to B10 mice (Goudemant *et al.*, 1998). In DMD patients and mdx mice, some types of molecules in the skeletal muscle, such as creatine kinase and myoglobin, are reported to be released into the bloodstream through microlesions in the sarcolemma (Ebashi *et al.,* 1959; Hooshmand, 1975; Ando *et al.*, 1978). It is therefore presumed that the leakage of intracellular Pi was likely the source of the elevated serum Pi observed in the mdx mice. Renal failure in mdx mice caused by dystrophin deficiency was unlikely, because the concentrations of serum creatinine and blood urea nitrogen were not significantly different between the mdx and normal mice (Brazeau *et al.*, 1992).

Inflammation and calcification: cause or effect?

In recent studies, inflammation has been proposed as a key factor in the pathogenesis of muscular dystrophy. Though the primary cause of DMD is dystrophin deficiency, the immune response elicited by membrane damage results in the progression of the disease (Tidball and Wehling-Henricks, 2005; Acharyya *et al.*, 2007). The accumulation of macrophages observed around calcifications and muscle fibers undergoing calcification suggests that ectopic calcification is intimately related to inflammation in mdx mouse skeletal muscle. It is probable that calcification triggers inflammation, for it has been reported that calcium phosphate crystals consisting predominantly of HA induce a proinflammatory response in macrophages (Nadra *et al.*, 2005). We also cannot deny the possibility that calcification is regulated by macrophages, as it has been shown that activated monocytes and macrophages enhance the calcification of vascular smooth muscle cells by cell-cell interaction and the secretion of tumor necrosis factor-alpha, a pleiotropic cytokine known to promote vascular calcification (Tintut *et al.*, 2000; Tintut *et al.*, 2002). Whether or not calcification in mdx mouse skeletal muscle induces inflammation has yet to be clarified, and is a topic for future studies.

Conclusion

The goal of this study was to investigate the mechanisms of ectopic calcification operating in mdx mouse skeletal muscle. Given the results of the experiments described above, we conclude that Pi and calcium deposits induce osteogenesis in myoblasts resulting in calcification, while calcification may also be generated passively by the elevation of intracellular Pi and calcium ion levels. A hypothetical model of ectopic calcification in mdx skeletal muscle is presented in Fig. 9.

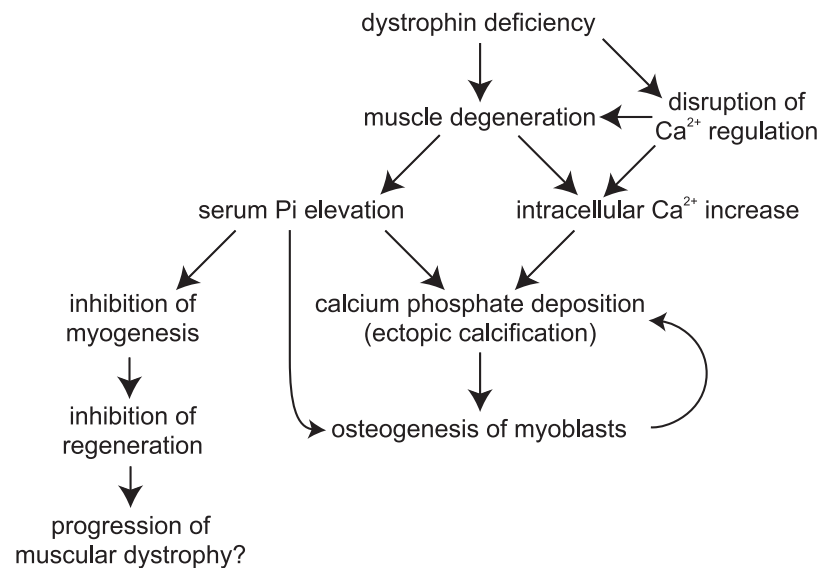Ectopic calcification can be observed easily using X-ray

Fig. 9. Hypothetical mechanism of ectopic calcification in mdx mouse skeletal muscle. Leakage of Pi from degenerated fibers elevates the serum Pi, inducing osteogenesis and calcification in myoblasts. Meanwhile, calcium regulation is disrupted in dystrophin-deficient muscle fibers, causing an increase in intracellular calcium. Pi and calcium ions form calcium phosphate precipitates. Calcium depositions induce osteogenesis in myoblasts, thus creating a positive feedback loop of osteogenesis and calcification. In addition, elevated Pi levels inhibit myogenesis, and the decrease of cells committed to myogenesis inhibits muscle regeneration which leads to the progression of DMD.

CT and other techniques, without the need for biopsy or near-infrared fluorescence imaging methods (Zaheer *et al.*, 2001). The possibility of monitoring ectopic calcification non-invasively in mdx mice provides a novel means of diagnosis and evaluation of therapeutic treatments for DMD.

To our knowledge, this study is the first attempt to comprehensively describe ectopic calcification in mdx mouse skeletal muscle and elucidate the mechanisms underlying the phenomenon (Fig. 9). In addition, although growth factor-mediated osteoinduction is already known, this is the first report to suggest that the calcification of skeletal muscle cells is caused by elevated Pi levels. We expect that our findings will offer novel insight into ectopic calcification in skeletal muscle and lead to an improved understanding of the pathology and therapy of muscular dystrophy.

References

Acharyya, S., Villalta, S., Bakkar, N., Bupha-Intr, T., Janssen, P., Carathers, M., Li, Z., Beg, A., Ghosh, S., Sahenk, Z., Weinstein, M., Gardner, K., Rafael-Fortney, J., Karin, M., Tidball, J., Baldwin, A., and Guttridge, D. 2007. Interplay of IKK/NF-kappaB signaling in macrophages and myofibers promotes muscle degeneration in Duchenne muscular dystrophy. *J. Clin. Invest.*, **117**: 889–901.

Ando, T., Shimizu, T., Kato, T., Ohsawa, M., and Fukuyama, Y. 1978. Myoglobinemia in children with progressive muscular dystrophy. *Clin. Chim. Acta*, **85**: 17–22.

Asakura, A., Komaki, M., and Rudnicki, M. 2001. Muscle satellite cells are multipotential stem cells that exhibit myogenic, osteogenic, and adipogenic differentiation. *Differentiation*, **68**: 245–253.

Berchtold, M., Brinkmeier, H., and Müntener, M. 2000. Calcium ion in skeletal muscle: its crucial role for muscle function, plasticity, and disease. *Physiol. Rev.*, **80**: 1215–1265.

Blake, D., Weir, A., Newey, S., and Davies, K. 2002. Function and genetics of dystrophin and dystrophin-related proteins in muscle. *Physiol. Rev.*, **82**: 291–329.

Blau, H., Chiu, C., and Webster, C. 1983. Cytoplasmic activation of human nuclear genes in stable heterocaryons. *Cell*, **32**: 1171–1180.

Brazeau, G., Mathew, M., and Entrikin, R. 1992. Serum and organ indices of the mdx dystrophic mouse. *Res. Commun. Chem. Pathol. Pharmacol.*, **77**: 179–189.

Bulfield, G., Siller, W., Wight, P., and Moore, K. 1984. X chromosome-linked muscular dystrophy (mdx) in the mouse. *Proc. Natl. Acad. Sci. USA*, **81**: 1189–1192.

Damien, C. and Parsons, J. 1991. Bone graft and bone graft substitutes: a review of current technology and applications. *J. Appl. Biomater.*, **2**: 187–208.

Davie, J., Cho, J., Meadows, E., Flynn, J., Knapp, J., and Klein, W. 2007. Target gene selectivity of the myogenic basic helix-loop-helix transcription factor myogenin in embryonic muscle. *Dev. Biol.*, **311**: 650–664.

Desbois, C., Hogue, D.A., and Karsenty, G. 1994. The mouse osteocalcin

gene cluster contains three genes with two separate spatial and temporal patterns of expression. *J. Biol. Chem.*, **269**: 1183–1190.

Ebashi, S., Toyokura, Y., Momoi, H., and Sugita, H. 1959. High creatine phosphokinase activity of sera of progressive muscular dystrophy. *J. Biochem.*, **46**: 103–104.

Ervasti, J., Ohlendieck, K., Kahl, S., Gaver, M., and Campbell, K. 1990. Deficiency of a glycoprotein component of the dystrophin complex in dystrophic muscle. *Nature*, **345**: 315–319.

Ferguson, J., Richard, J., O'Laughlin, J., and Banks, C. 1964. Simultaneous Spectrophotometric Determination of Calcium and Magnesium with Chlorophosphonazo III. *Analytical Chemistry.*, **36**: 796–799.

Geissinger, H., Rao, P., and McDonald-Taylor, C. 1990. "mdx" mouse myopathy: histopathological, morphometric and histochemical observations on young mice. *J. Comp. Pathol.*, **102**: 249–263.

Giachelli, C. 1999. Ectopic calcification: gathering hard facts about soft tissue mineralization. *Am. J. Pathol.*, **154**: 671–675.

Gillis, J. 1999. Understanding dystrophinopathies: an inventory of the structural and functional consequences of the absence of dystrophin in muscles of the mdx mouse. *J. Muscle Res. Cell Motil.*, **20**: 605–625.

Gindler, E. and King, J. 1972. Rapid colorimetric determination of calcium in biologic fluids with methylthymol blue. *Am. J. Clin. Pathol.*, **58**: 376–382.

Goudemant, J.F., Deconinck, N., Tinsley, J.M., Demeure, R., Robert, A., Davies K.E., and Gillis, J.M. 1998. Expression of truncated utrophin improves pH recovery in exercising muscles of dystrophic mdx mice: a 31P NMR study. *Neuromuscular Disord.*, **8**: 371–379.

Hoffman, E., Brown, R.J., and Kunkel, L. 1987. Dystrophin: the protein product of the Duchenne muscular dystrophy locus. *Cell*, **51**: 919–928.

Hooshmand, H. 1975. Serum lactate dehydrogenase isoenzymes in neuromuscular diseases. *Dis. Nerv. Syst.*, **36**: 607–611.

Hwang, W. and Cha, S. 1973. A new enzymatic method for the determination of inorganic phosphate and its application to the nucleoside diphosphatase assay. *Anal. Biochem.*, **55**: 379–387.

Jono, S., McKee, M., Murry, C., Shioi, A., Nishizawa, Y., Mori, K., Morii, H., and Giachelli, C. 2000. Phosphate regulation of vascular smooth muscle cell calcification. *Circ. Res.*, **87**: E10–E17.

Katagiri, T., Yamaguchi, A., Komaki, M., Abe, E., Takahashi, N., Ikeda, T., Rosen, V., Wozney, J., Fujisawa-Sehara, A., and Suda, T. 1994. Bone morphogenetic protein-2 converts the differentiation pathway of C2C12 myoblasts into the osteoblast lineage. *J. Cell Biol.*, **127**: 1755–1766.

Ketteler, M., Westenfeld, R., Schlieper, G., and Brandenburg, V. 2005. Pathogenesis of vascular calcification in dialysis patients. *Clin. Exp. Nephrol.*, **9**: 265–270.

Kuro-o, M., Matsumura, Y., Aizawa, H., Kawaguchi, H., Suga, T., Utsugi, T., Ohyama, Y., Kurabayashi, M., Kaname, T., Kume, E., Iwasaki, H., Iida, A., Shiraki-Iida, T., Nishikawa, S., Nagai, R., and Nabeshima, Y.I. 1997. Mutation of the mouse klotho gene leads to a syndrome resembling ageing. *Nature*, **390**: 45–51.

Li, X. and Giachelli, C. 2007. Sodium-dependent phosphate cotransporters and vascular calcification. *Curr. Opin. Nephrol. Hypertens.*, **16**: 325–328.

Li, X., Yang, H.Y., and Giachelli, C.M. 2008. BMP-2 promotes phosphate uptake, phenotypic modulation, and calcification of human vascular smooth muscle cells. *Atherosclerosis*, **199**: 271–277.

Lievremont, M., Potus, J., and Guillou, B. 1982. Use of alizarin red S for histochemical staining of Ca^{2+} in the mouse; some parameters of the chemical reaction *in vitro*. *Acta Anat (Basel).*, **114**: 268–280.

Matsuda, R., Nishikawa, A., and Tanaka, H. 1995. Visualization of dystrophic muscle fibers in mdx mouse by vital staining with Evans blue: evidence of apoptosis in dystrophin-deficient muscle. *J. Biochem.*, **118**: 959–964.

Murshed, M., Harmey, D., Millán, J.L., McKee, M.D., and Karsenty, G. 2005. Unique coexpression in osteoblasts of broadly expressed genes accounts for the spatial restriction of ECM mineralization to bone. *Genes Dev.*, **19**: 1093–1104.

Nadra, I., Mason, J., Philippidis, P., Florey, O., Smythe, C., McCarthy, G., Landis, R., and Haskard, D. 2005. Proinflammatory activation of macrophages by basic calcium phosphate crystals via protein kinase C and MAP kinase pathways: a vicious cycle of inflammation and arterial calcification? *Circ. Res.*, **96**: 1248–1256.

Nguyen, F., Cherel, Y., Guigand, L., Goubault-Leroux, I., and Wyers, M. 2002. Muscle lesions associated with dystrophin deficiency in neonatal golden retriever puppies. *J. Comp. Pathol.*, **126**: 100–108.

Perry, R. and Rudnick, M. 2000. Molecular mechanisms regulating myogenic determination and differentiation. *Front. Biosci.*, **5**: D750–D767.

Petrof, B., Shrager, J., Stedman, H., Kelly, A., and Sweeney, H. 1993. Dystrophin protects the sarcolemma from stresses developed during muscle contraction. *Proc. Natl. Acad. Sci. USA*, **90**: 3710–3714.

Ploszaj, T., Motyl, T., Orzechowski, A., Zimowska, W., Wareski, P., Skierski, J., and Zwierzchowski, L. 1998. Antiapoptotic action of prolactin is associated with up-regulation of Bcl-2 and down-regulation of Bax in HC11 mouse mammary epithelial cells. *Apoptosis*, **3**: 295–304.

Schinke, T. and Karsenty, G. 2000. Vascular calcification—a passive process in need of inhibitors. *Nephrol. Dial. Transplant.*, **15**: 1272–1274.

Sitara, D., Razzaque, M.S., Hesse, M., Yoganathan, S., Taguchi, T., Erben, R.G., Juppner, H., and Lanske, B. 2004. Homozygous ablation of fibroblast growth factor-23 results in hyperphosphatemia and impaired skeletogenesis, and reverses hypophosphatemia in Phex-deficient mice. *Matrix Biol.*, **23**: 421–432.

Stubbs, J.R., Liu, S., Tang, W., Zhou, J., Wang, Y., Yao, X., and Quarles, L.D. 2007. Role of hyperphosphatemia and 1,25-dihydroxyvitamin D in vascular calcification and mortality in fibroblastic growth factor 23 null mice. *J. Am. Soc. Nephrol.*, **18**: 2116–2124.

Tan, Y., Wang, G., Fan, H., Wang, X., Lu, J., and Zhang, X. 2007. Expression of core binding factor 1 and osteoblastic markers in C2C12 cells induced by calcium phosphate ceramics *in vitro*. *J. Biomed. Mater. Res. A.*, **82**: 152–159.

Tidball, J. and Wehling-Henricks, M. 2005. Damage and inflammation in muscular dystrophy: potential implications and relationships with autoimmune myositis. *Curr. Opin. Rheumatol.*, **17**: 707–713.

Tintut, Y., Patel, J., Parhami, F., and Demer, L. 2000. Tumor necrosis factor-alpha promotes *in vitro* calcification of vascular cells via the cAMP pathway. *Circulation*, **102**: 2636–2642.

Tintut, Y., Patel, J., Territo, M., Saini, T., Parhami, F., and Demer, L. 2002. Monocyte/macrophage regulation of vascular calcification *in vitro*. *Circulation*, **105**: 650–655.

Wada, M., Inagawa-Ogashiwa, M., Shimizu, S., Yasumoto, S., and Hashimoto, N. 2002. Generation of different fates from multipotent muscle stem cells. *Development*, **129**: 2987–2995.

Xiao, Z.S., Hinson, T.K., and Quarles, L.D. 1999. Cbfa1 isoform overexpression upregulates osteocalcin gene expression in non-osteoblastic and pre-osteoblastic cells. *J. Cell Biochem.*, **74**: 596–605.

Yaffe, D. and Saxel, O. 1977. Serial passaging and differentiation of myogenic cells isolated from dystrophic mouse muscle. *Nature*, **270**: 725–727.

Yoshiko, Y., Candeliere, G., Maeda, N., and Aubin, J. 2007. Osteoblast autonomous Pi regulation via Pit1 plays a role in bone mineralization. *Mol. Cell Biol.*, **27**: 4465–4474.

Zaheer, A., Lenkinski, R., Mahmood, A., Jones, A., Cantley, L., and Frangioni, J. 2001. *In vivo* near-infrared fluorescence imaging of osteoblastic activity. *Nat. Biotechnol.*, **19**: 1148–1154.

Zaidi, S.K., Javed, A., Choi, J.Y., van Wijnen, A.J., Stein, J.L., Lian, J.B., and Stein, G.S. 2001. A specific targeting signal directs Runx2/Cbfa1 to subnuclear domains and contributes to transactivation of the osteocalcin gene. *J. Cell Sci.*, **114**: 3093–3102.